THE ASTRONOMICAL JOURNAL VOLUME 90, NUMBER 3 MARCH 1985

THE STATISTICAL DISTRIBUTION OF THE NEUTRAL-HYDROGEN CONTENT OF ELLIPTICAL GALAXIES

G. R. KNAPP, EDWIN L. TURNER,[a] AND P. E. CUNNIFFE
Department of Astrophysical Sciences, Princeton University, Princeton, New Jersey 08544
Received 15 October 1984

ABSTRACT

We have examined the form of the distribution function for the relative H I content, $M_{\rm H\,I}/L_B$, of elliptical galaxies, using a data set derived from all recent H I observations of ellipticals in the literature. The characteristics of this combined data set are poorly defined, but upon examination it appears to be reassuringly free of built-in biases and correlations. The data set contains 152 galaxies; 23 of these have been detected in the H I line. The detected galaxies are shown to be more H I rich on average than the galaxies in the whole sample. A method for recovering the intrinsic distribution of $M_{\rm H\,I}/L_B$, using both detection and upper-limit data, is described, and the data are shown to be consistent with a shallow power-law differential distribution $N\sim(M_{\rm H\,I}/L_B)^{-1.5}$. This distribution is quite different from that for spirals, where $N(M_{\rm H\,I}/L_B)$ has a well-defined mean value and a small dispersion. This result strongly suggests that the gas and star contents of ellipticals are decoupled, i.e., the gas has an external origin.

I. INTRODUCTION

Do elliptical galaxies contain cold gas? Until recently, the answer to this question was thought to be negative. The global H I content for galaxies, measured using the 21-cm line, was found to be a function of morphological type (e.g., Roberts 1975), with the later types having larger relative gas contents. Ellipticals were not detected in the H I line, at sensitivity levels of about one-tenth of the H I content of large spirals. While these results are consistent with expectations based on the low angular momentum and old stellar populations characteristic of ellipticals, some questions remained. For example, a minority ($\sim$20%) of ellipticals have central H II regions (e.g., Humason, Mayall, and Sandage 1956), and a similar fraction show the presence of active nuclear radio sources (e.g., Hummel 1980). Further, the interstellar medium in ellipticals should be replenished by gas lost by the evolving stellar population (e.g., Faber and Gallagher 1976). More sensitive searches for H I in ellipticals, prompted by these questions, finally led to the detection of small amounts of H I (typically, a few $\times 10^8\,M_\odot$) in several nearby galaxies, including the active ellipticals NGC 1052 and NGC 4278 (Bottinelli and Gouguenheim 1977a; Gallagher *et al.* 1977; Whiteoak and Gardner 1977; Knapp, Gallagher, and Faber 1978; Fosbury *et al.* 1978).

Most ellipticals remain undetected in the H I line. The form of the distribution of M (H I) or M (H I)/L_B is of interest for considerations of the origin of the gas. The low detection rate led to the suggestion that the distribution is bimodal, i.e., most ellipticals contain little if any gas, while those which do are unusually gas rich. A statistical analysis by Sanders (1980) showed that the available data were consistent with such a distribution.

There have been several observational developments since Sanders' work which make reanalysis of the data worthwhile. First, continued observations have better clarified and defined those galaxies which are reliably detected in the H I line. When the amount of gas present is so small, and the detection level only a few times the observational noise, it is inevitable that the H I properties of an individual galaxy can be ill defined. Observations made with several different telescopes now exist for many galaxies, allowing a better evaluation of their H I content. Second, there has been the recognition that some I0 galaxies, such as NGC 5128, are likely to belong to the class of ellipticals containing H I—these galaxies have dust lanes but no stellar disks (see, e.g., the discussion by Hawarden *et al.* 1982). Third, Haynes and Giovanelli (1980), in their investigation of isolated galaxies, have found that the few early-type members of this class tend to be gas rich. Fourth, many dwarf ellipticals have now been observed, with detections of H I in several (Johnson and Gottesman 1983; Lake and Schommer 1984). These observations have greatly extended the luminosity range of ellipticals which have been searched for gas, and have also increased the sample of well-observed ellipticals by about a factor of 3 over that analyzed by Sanders. Nevertheless, in the present sample, as in that discussed by Sanders, most of the ellipticals remain undetected in the H I line.

For these reasons, we have undertaken a reanalysis of the H I observations of elliptical galaxies. The currently available data are rather heterogeneous in sensitivity, etc., so the work presented here is twofold. First, the data set, gathered from the literature, is described. Most of the details of the data for individual galaxies, and of the reduction of the data, are given in Appendices A–C, with the data set analyzed in this paper presented in Table II. The data are briefly discussed in Sec. II, where the completeness, sensitivity, and selection biases are examined. Second, the analysis of the data and the evaluation of the distribution function $\phi\,[M\,(\mathrm{H\,I})/L_B]$ are described in Sec. III. We find that, while the data do not rule out a bimodal distribution, they do not suggest one. The data set is better described by an approximately power-law distribution in $M_{\rm H\,I}/L_B$. This result is discussed in Sec. IV, where it is compared with the distribution of H I for a sample of spirals. The implications of our results for the origin of H I in ellipticals, and the conclusions of this work, are also presented in Sec. IV.

II. THE DATA

The data set used in this study was culled from the litera-

[a] Alfred P. Sloan Research Fellow.

 0004-6256/85/030454-15$00.90

ture published since 1975. At that time, sensitive receivers began to be used on the large centimeter-wavelength telescopes, and the first detections of H I in ellipticals came soon afterwards. The literature compilation by Huchtmeier *et al.* (1983) was of great value in the data search.

The data are listed in Table II and described in detail in Appendix A. The final list contains a total of 152 galaxies, with 23 H I detections and 129 nondetections; this sample is about three times as large as that analyzed by Sanders (1980). Some of the galaxies are suspected or known not to be ellipticals; these include the Sombrero galaxy NGC 4594 and the E/SO galaxy NGC 3998. The justification for including these and other galaxies is given in Appendix A; the analysis in the next section will be carried out with and without these galaxies.

For all the galaxies in Table II, the blue luminosity L_B has been calculated following the prescriptions of de Vaucouleurs, de Vaucouleurs, and Corwin (1976; hereafter referred to as RC2). The corrections applied to the magnitudes are described in Appendix A and the distance calculation [based on the Aaronson *et al.* (1982) model for the infall of the Local Group towards Virgo and a Hubble constant of 100 km/s/Mpc] is described in Appendix B. For the galaxies in which H I has been detected, we calculate the H I mass using

$$M(\text{H I}) = 2.36\times 10^5 D^2 FI \quad M_\odot, \tag{1}$$

where D is the distance in Mpc and FI the integrated flux in the H I line in units of Jy km/s. We have also calculated the minimum mass M_u which could have been detected in the observation, with the quantity FI in equation (1) replaced by $3\sigma_{\rm rms}$, where $\sigma_{\rm rms}$ is the rms noise of the observation and ΔV is the observed linewidth in km/s. Most of the analysis in the next section is based on the distance-independent ratios $r = M(\text{H I})/L_B$ and $r_u = M_u(\text{H I})/L_B$.

For the upper limits in Table II, we have calculated values of M_u(H I) and r_u as above, but a value of ΔV must be assumed. As shown by several authors (Faber and Jackson 1976; Tully and Fisher 1977), the linewidth scales with luminosity for galaxies of all morphological types. In Appendix C, we plot ΔV (the full width of the H I line at half power) versus the luminosity for the H I-detected ellipticals. The data are consistent with a relationship $\Delta v \sim L_B^{1/3}$, which is used in estimating ΔV for the undetected galaxies. These values of ΔV are used in calculating the values of M_u(H I) and r_u for the nondetected galaxies in Table II. For the upper limits, then, r_u is no longer distance independent but is proportional to $D^{2/3}$, so the data could contain distance-dependent biases.

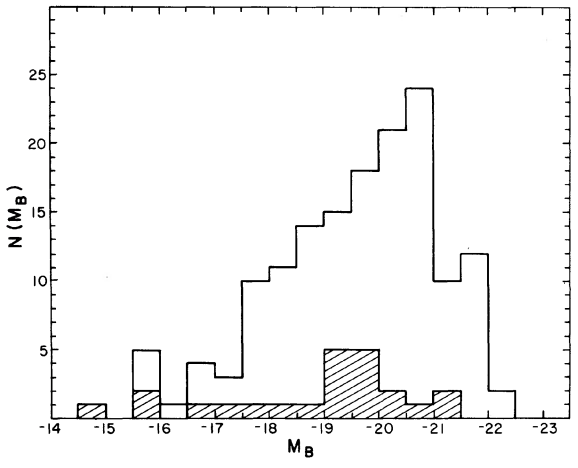

FIG. 1. Distribution of absolute blue magnitudes M_B for the elliptical galaxy sample. The galaxies in which H I has been detected are shaded.

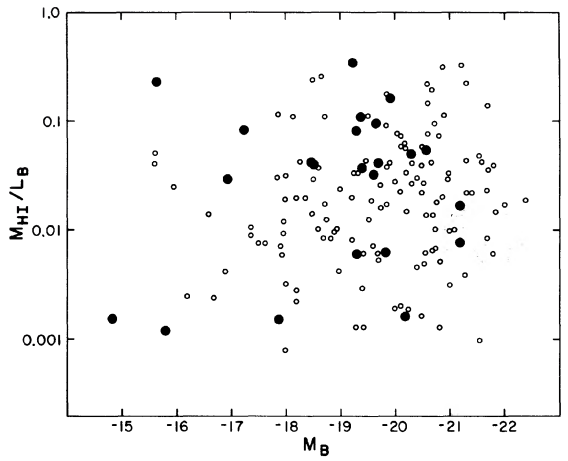

FIG. 2. Plot of $M_{\rm H\,I}/L_B$ in $M_\odot/L_\odot$, or its upper limit, versus absolute blue magnitude M_B for the elliptical galaxy sample. The detections are plotted as dark circles; the upper limits (from Table II) as light circles.

These calculations of Δv implicitly assume that the H I structure in the undetected galaxy is edge-on. For the analysis described in the next section of this paper, we calculated several further data sets, valid only for statistical purposes, in which the imagined H I structure in each galaxy was given a random inclination. The linewidth so calculated was constrained always to be greater than 60 km/s, because even face-on galaxies are observed to have H I lines of about this width or greater, due to internal turbulence in the gas, warping in the galaxy, and instrumental resolution. In the subsequent analysis, these various "random" data sets were found to give results which were identical to well within the uncertainties.

The adopted data set contains the most sensitive observation made for each galaxy. Some of the upper limits $r_u = M_u(\text{H I})/L_B$ were found to be larger than any of the detected values, and the corresponding galaxies were removed from the sample.

Figure 1 shows the distribution of the absolute blue magnitude M_B both for the total sample and for the ellipticals in which H I has been detected. The histogram for the total data set bears a reasonable resemblance to that produced by a magnitude-limited sample of the luminosity function (e.g., Schechter 1976). Further, apart from the galaxies fainter than $-16^{\rm m}$, the galaxies in which H I has been detected have roughly the same distribution of M_B as do those in which no detection has been made, and thus the H I-detected galaxies are also a fair sample of the luminosity function.

In Fig. 2, we show the plot of $M_{\rm H\,I}/L_B$ versus M_B. The observed values of $M_{\rm H\,I}/L_B$ are plotted for the detected galaxies, and the upper limits from Table II for the undetected galaxies. The quantities are completely uncorrelated for either subset of the data, and there are thus no obvious built-in correlations to be taken into account when we examine the distribution of $M_{\rm H\,I}/L_B$.

Next, in Figs. 3 and 4, we show the histograms of r_u, for three samples: (1) the H I-detected galaxies (here, r_u is the

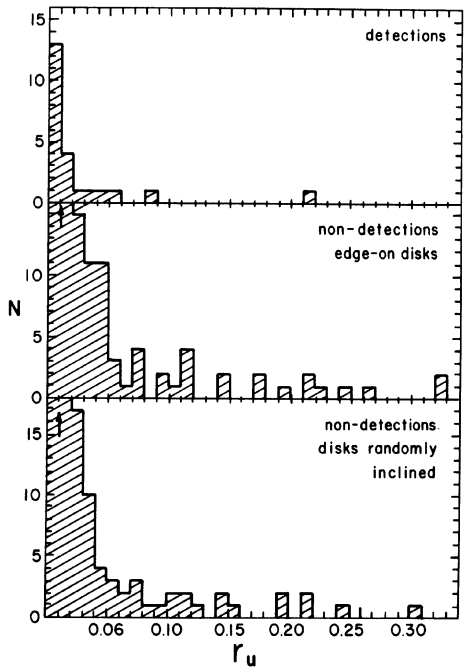

FIG. 3. Histograms of r_u, the observational sensitivity (upper limit) of M_{H_I}/L_B, for (a) H I-detected ellipticals (upper panel), (b) nondetected ellipticals, edge-on disks assumed (center panel)—see the text and Table II, (c) nondetected ellipticals with randomly oriented disks assumed (see the text) (lower panel). The histograms cover the whole observed range of r_u, 0–0.3 $M_\odot/L_\odot$.

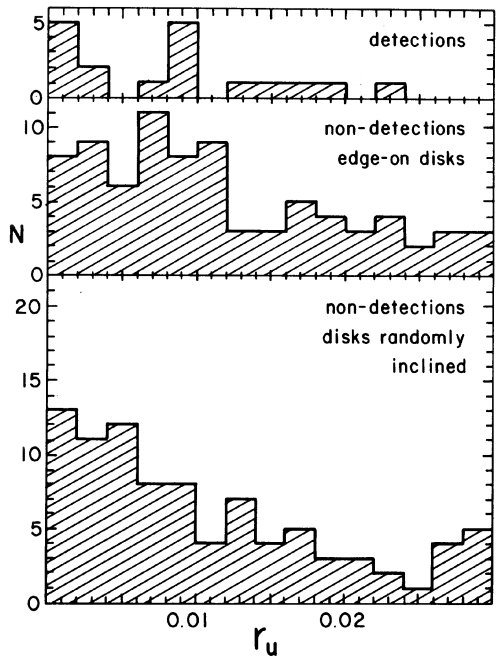

FIG. 4. As for Fig. 3, for small values of r_u, 0–0.03 $M_\odot/L_\odot$.

minimum amount of H I which could have been detected in the observation), (2) the nondetected galaxies, with edge-on H I disks assumed and (3) the nondetected galaxies with the H I disks assumed to be randomly inclined. The distribution of r_u for the detections is similar to that of the nondetections and covers a similar range of values. Thus, in terms of the values of M(H I)/L_B, the detected galaxies have been observed over a range of sensitivities similar to that for the nondetected galaxies.

The analogous histograms for M_u(H I) are shown in Fig. 5. Here, the distributions are again similar except for the VLA observations of the Local Group dwarf ellipticals by Johnson and Gottesman (1983). Figures 1–5 thus show that, apart from dwarf ellipticals, the galaxies in which H I has been detected are a fair subsample, both optically and in terms of the sensitivity of the H I observations, of the total. (The Johnson and Gottesman observations are consistent with the presently untestable hypothesis that all dwarf ellipticals contain a small amount of gas.) We can thus ask the question: are the H I-detected galaxies also a fair sample of the whole in terms of r ($\equiv M$(H I)/L_B), or do they have higher values of r than the rest of the sample?

The histograms of r and of M(H I) for the 23 detected galaxies are shown in Figs. 6 and 7. The mean value of r for these 23 galaxies is 0.06 $M_\odot/L_\odot$. We now test the hypothesis that the distribution of r for all the galaxies is the same as that shown in Fig. 6, as follows.

We assume that all the galaxies belong to this distribution, and "observe" them with the sensitivities of the observations. That is, we assume that each galaxy is drawn from the distribution in Fig. 6 and compare each value of r with the values of r_u for all the galaxies; if $r > r_u$, the galaxy is "detected". The resulting data set contains 90 detections and 62 upper limits; this result is little changed if the upper limits with randomly inclined disks are used, or if the distribution in Fig. 6 is smoothed. This exercise thus confirms the impression gained from Figs. 3, 4, and 6; if all of the galaxies belong to the distribution in Fig. 6, the observations are sensitive enough to have detected the majority of them, and thus the undetected galaxies must have M(H I)/L_B values substantially smaller than those of the detected galaxies.

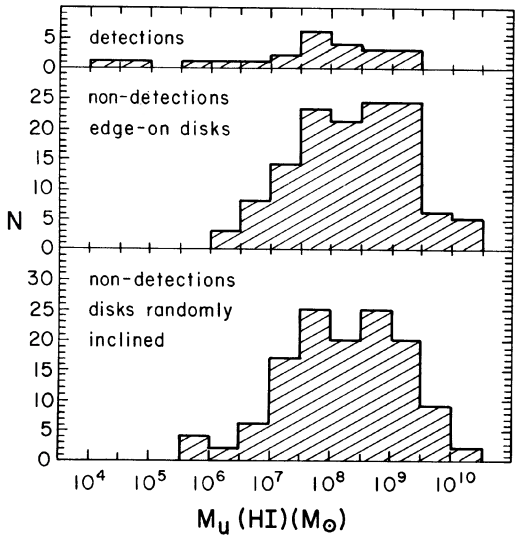

FIG. 5. Histogram of M_u (H I), the observational sensitivity (upper limit) for H I observations of ellipticals in $M_\odot$, for three samples, as in Fig. 3.

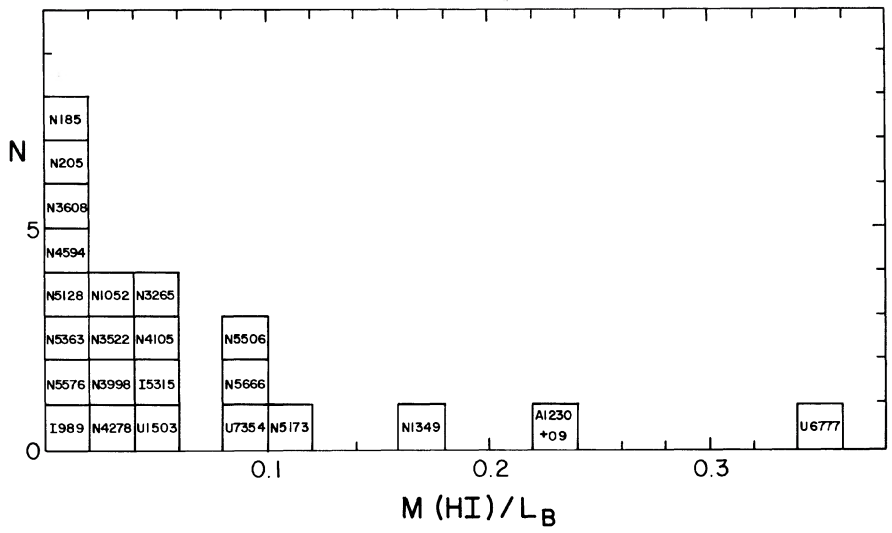

FIG. 6. Histogram of $r = M_{\rm H\,I}/L_B$ $(M_\odot/L_\odot)$ for H I-detected ellipticals.

We can next assume that some of the galaxies belong to the distribution in Fig. 6, while the remainder have $r = 0$ (a simple bimodal distribution). Repeating the above test, we now find that the observations are consistent with 35 galaxies having values of r lying in the observed distribution of detections, while the remainder (117 galaxies) have $r = 0$. At first sight, this result appears to confirm the suggestion that the distribution of H I in ellipticals is bimodal. Note, however, that we have only shown that such a model could explain the data, not that it is required by the data; we have only shown that the detected galaxies are on the whole more gas rich than average. In the next section, we discuss a model-independent method for deriving the functional form of $\phi(r)$, and use it to derive the intrinsic distribution of $M_{\rm H\,I}/L_B$.

III. THE DISTRIBUTION FUNCTION OF M(H I)/L_B IN ELLIPTICALS

In this section, we shall attempt to recover the intrinsic distribution of $r = m$(H I)/L_B from the observed distribution and nondetections described in Sec. II and given in Table II. Obviously, this is not necessarily possible given the poorly defined nature of the data sample which has accumulated in the literature. An examination of the data is reassuring, however. Note that observed values of, and upper limits on, r are uncorrelated with L_B, suggesting that biases in the apparent-magnitude distribution of observed galaxies will not bias the r distribution. In any case, as discussed in Sec. II, the distribution of absolute magnitudes for both the detected and the undetected galaxies resembles that expected for a fair apparent-magnitude-limited sample. Finally, we saw in Sec. II that the limiting r sensitivities were distributed similarly for both the detected and undetected galaxies, thus suggesting that the actual detections occurred in a fair subsample of the objects observed. These facts do not prove that the sample given in Table II is a fair and unbiased sampling of the intrinsic r distribution but they are consistent with and supportive of such a contention; we will thus proceed on the basis of a fair-sampling assumption.

To be explicit, we assume that each observation in Table II represents one random sampling of the intrinsic r distribution in the range of r values from the limiting r sensitivity observed up to infinity. Thus the number of observations with limiting sensitivities smaller than any particular r value is the number of times this data set has sampled the distribution at r. This statement of our assumption suggests a straightforward technique for removing the selection bias from the distribution of actual detections in order to estimate

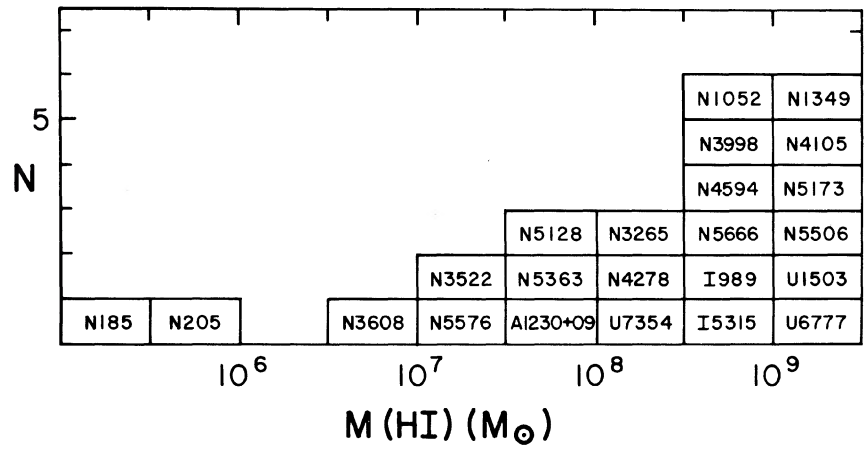

FIG. 7. Histogram of $M_{\rm H\,I}$ $(M_\odot)$ for H I-detected ellipticals.

the intrinsic r distribution, namely that each detection be assigned a weight equal to the ratio of the total number of observations to the number of observations which were in fact sensitive enough to have actually made the detection. This technique may be described more fully by Turner (1985).

In other words, let $P(r)dr$ be the intrinsic probability of r values and $N(r)dr$ the observed distribution of the detections among the T observations; then we have

$$P(r)dr = N(r)dr/L\,(<r), \tag{2}$$

where $L\,(<r)$ is the number of the observations (detections or nondetections) for which the limiting detectable r value is less than or equal to r. Of course, in practice, this procedure must be carried out using finite-width Δr bins rather than infinitesimal dr values. This is best accomplished as indicated above by calculating weights $[T/L\,(<r)]$ for each observed point and then summing these weights over finite r bins.

The technique described above is very similar in spirit to the $1/V_{\max}$ estimator of luminosity functions (Schmidt 1968; Felten 1976; Bahcall 1980). It differs from this better-known approach in that it is applicable to samples which are defined in terms of a particular set of specific objects instead of in terms of a set of all objects satisfying some predefined selection criteria and in that it produces intrinsic probability density distributions rather than volume density distributions.

This procedure was applied to the data set given in Table II, and the resulting estimates of the intrinsic r distribution are given in Table I in the form of $P(r)\Delta$ (log (r)). In addition to the basic version of the data described in Sec. II, two further data sets were also analyzed. These results are also shown in Table I and refer on the one hand to the addition of the galaxy NGC 4594 to the basic sample and on the other hand to the elimination of all galaxies with morphological classifications which are in any way uncertain or peculiar. The results for these alternate data sets are not significantly different from those for the basic data set, so they will therefore be disregarded in further discussions. The errors associated with each point in Table I are the square root of the sum of the squares of the weights of the points contributing to that bin. The point corresponding to $\log r < -3$ in Table I is calculated by requiring the integral over $P(r)dr$ to be unity.

Figure 8 is a plot of the $P(r)dr$ distribution as given in Table I derived from the basic data set; it includes a weighted least-squares best-fitting power law. This power law corresponds to

$$\log\,[N(r)dr] = [\,-(1.9 \pm 0.2) - (1.48 \pm 0.13)\log r]dr, \tag{3}$$

which can be usefully approximated by a $-3/2$ index but obviously can not be extrapolated all the way to $r = 0$ due to its divergence. The power-law fit is acceptable but not particularly excellent; the null hypothesis probability associated with the reduced χ^2 of this fit is about 0.12. There is no apparent evidence for a bimodal distribution, though the (insignificantly) high point at $\log r = -1.5$ to -1 may be the remnant of the effect seen by Sanders (1980).

IV. DISCUSSIONS AND CONCLUSIONS

a) The Origin of H I in Elliptical Galaxies

The distribution of $M(\text{H I})/L_B$ presented in Fig. 8 for elliptical galaxies is best described by a power law. The concept of a mean value of $M(\text{H I})/L_B$ is thus ill defined. Most ellipticals have $M(\text{H I})/L_B < 10^{-3}\,M_\odot/L_\odot$. At this level, most galaxies are undetectable at present instrumental-sensitivity levels. In practical terms, also, such small amounts of gas may be distributed over the large volume of the galaxy, at very low densities. Then, either the gas is of such low density that the 21-cm transition is no longer collisionally excited, or the gas is ionized by ultraviolet light from the stars in the elliptical galaxy.

The distribution of $M_{\text{H I}}/L_B$ may be contrasted with that in spirals. For example, in Fig. 9 we plot the histogram of $M_{\text{H I}}/L_B$ for Sc spirals. The data plotted in Fig. 9 are from

TABLE I. Distribution of $M_{\text{H I}}/L_B$ for elliptical galaxies.

	Sample 1		Sample 2		Sample 3	
$\langle\log \frac{M_{HI}}{L_B}\rangle$	$\log(\frac{N}{No})$	σ	$\log(\frac{N}{No})$	σ	$\log(\frac{N}{No})$	σ
<-3	-0.32	0.16	-0.34	0.18	-0.32	0.17
-2.75	-0.48	0.22	-0.46	0.22	-0.45	0.22
-2.25	-1.18	0.28	-1.19	0.25	-1.27	0.31
-1.75	-1.52	0.26	-1.52	0.25	-1.60	0.31
-1.25	-1.14	0.14	-1.15	0.15	-1.24	0.18
-0.75	-1.67	0.24	-1.68	0.25	-1.61	0.25
-0.25	-2.18	0.43	-2.18	0.43	-2.11	0.43

Sample 1: Full sample (Table A.1)

Sample 2: Full sample minus NGC4594

Sample 3: Full sample minus NGC4594, possible SOs and blue compact galaxies (see text).

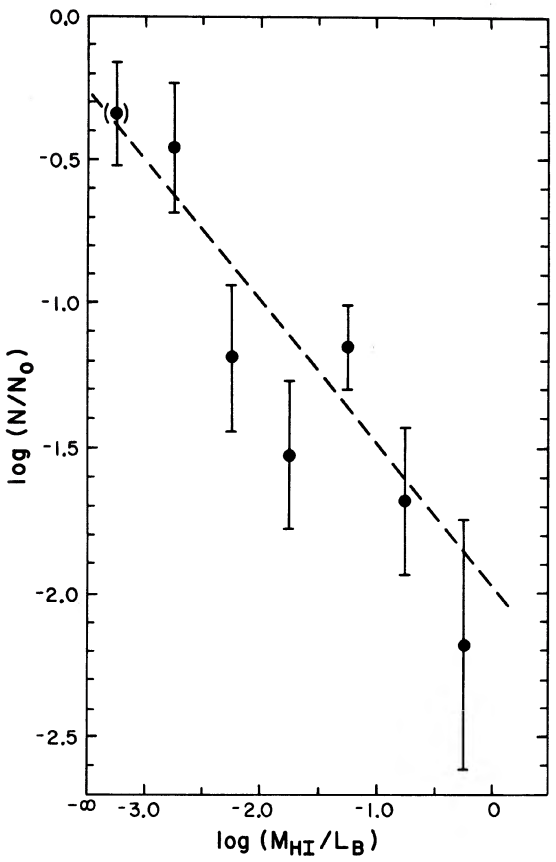

FIG. 8. Derived normalized distribution of M_{H_I}/L_B for elliptical galaxies. The dotted line shows a power-law fit to the data (see the text).

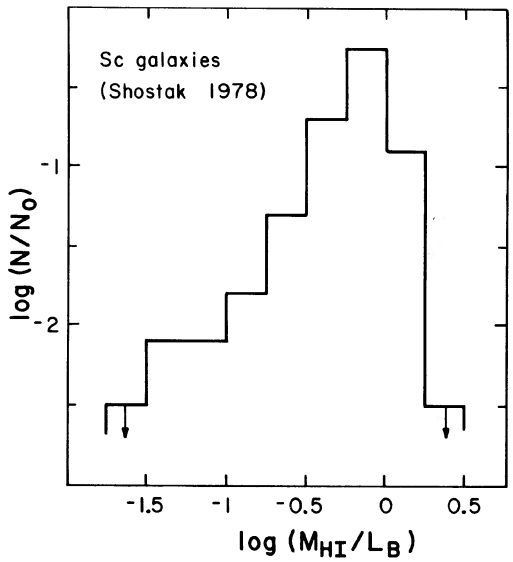

FIG. 9. Normalized distribution of M_{H_I}/L_B for Sc galaxies, from the sample of Shostak (1978).

the H I observations of late-type galaxies by Shostak (1978). Shostak's list contains 135 galaxies (a sample of size comparable to our sample of elliptical galaxies), with morphological types between Sbc and Scd. Of these galaxies, 124 were detected in the H I line. For the remaining 11, only four have known radial velocities and for these four, the typical upper limits for M_{H_I}/L_B are $\sim 0.05\, M_\odot/L_\odot$, similar to the lowest detected values. In any case, the number of nondetections is small enough to have little effect on the distribution, and the contribution of these galaxies was ignored. The histogram in Fig. 9 is then for the detections only.

The distribution function for Sc galaxies shown in Fig. 9 is quite unlike that for elliptical galaxies in Fig. 8, being narrow enough that it is reasonable to characterize it by a single mean value of M_{H_I}/L_B (cf. Roberts 1975). It is likely that much of the dispersion about the mean is due to observational uncertainties. The corrections applied to the magnitudes for internal and galactic observation are uncertain, the magnitudes themselves are subject to observational error, and the global H I fluxes, which in principle should be straightforward to measure, in practice are not. The H I disks for nearby galaxies are often partially resolved and uncertain correction factors must be applied (Fisher and Tully 1981), and edge-on galaxies have self-absorption in the H I line (Bajaja *et al.* 1984). Further, some spirals have been observed several times, and a comparison of observations in several different papers yields distressing discrepancies, sometimes up to a factor of 2, in the published line fluxes. The data of Fisher and Tully (1981) for Sc galaxies yields a distribution similar in shape to that in Fig. 9, but displaced in M_{H_I}/L_B. This displacement can probably be attributed to the different corrections applied to m_B by Fisher and Tully and by Shostak, who used the RC2 corrections.

Nevertheless, the distributions shown in Figs. 8 and 9 are quite different. They can not be directly compared because of stellar population differences—the blue light of ellipticals comes from evolving giants, while that from spirals is mostly due to young, hot main-sequence stars. For young populations, (L_*/M_*) is about three times higher than for old populations (Tinsley 1979). Taking this into account, we can see that the distributions in Figs. 8 and 9 overlap slightly—the ellipticals with the highest values of M_{H_I}/L_B ($\gtrsim 0.1\, M_\odot/L_\odot$) have relative H I contents as high as those of a few Sc galaxies, with M_{H_I}/L_B in the range ~ 0.03 to $0.1\, M_\odot/L_\odot$.

The small range of M_{H_I}/L_B for Sc galaxies (Fig. 9) clearly demonstrates the intimate relationship between the gas and stellar contents of spiral galaxies, and the effects of this relationship on galactic morphology, regardless of galactic luminosity. The situation is quite different in ellipticals—Fig. 8 suggests that the evolution of the gaseous and stellar populations in ellipticals have little to do with each other. In particular, it is likely that the gas in ellipticals has an external origin, either by slow accretion from the galaxy's surroundings, or by capture of a gas-rich companion. This conclusion is also supported by the observed spatial distribution of the H I in gas-rich ellipticals. Here, the spatial extent of the gas structures is usually larger than the optical extent of the galaxy, and the gas and stellar kinematics are very different (Raimond *et al.* 1981; Lake, Schommer, and van Gorkom 1984).

b) Conclusions

In this paper, we have presented an analysis of the H I content of elliptical galaxies. We find:

(1) Sensitive H I data exist for about 150 ellipticals, some

of uncertain morphology. Of these, 23 galaxies have been detected in the H I line.

(2) Examination of the data reveals no correlation between $M_{\rm H\,I}/L_B$ and L_B, nor any biases in the sensitivities used to observe the detected and nondetected galaxies. In addition, the galaxies (apart from dwarf ellipticals) seem to represent a fair magnitude-limited sample. The data thus appear to be free of obvious built-in biases and correlations.

(3) The ellipticals in which H I has been detected are H I rich relative to the remainder of the sample.

(4) The distribution of $M_{\rm H\,I}/L_B$ is roughly a power law between $\sim 10^{-3}\,M_\odot/L_\odot$ and $0.3\,M_\odot/L_\odot$, the range of the observations. The majority of ellipticals have $M_{\rm H\,I}/L_B < 10^{-3}\,M_\odot/L_\odot$. However, a bimodal distribution is not required by the data and the power-law distribution provides the best available fit.

(5) The distribution of $M_{\rm H\,I}/L_B$ in spirals has been examined for comparison. This distribution is roughly Gaussian in log r with a well-defined average value and small dispersion. Thus, for the ellipticals, in contrast to the spirals, the gas and light are uncorrelated.

(6) The nature of the distribution of M (H I)$/L_B$ for ellipticals strongly supports an external origin for the gas in elliptical galaxies.

This paper includes, in part, the results of P.E.C.'s A. B. Senior thesis at Princeton University. We are very grateful to J. E. Gunn and M. Schwarzschild for valuable discussions and to the National Science Foundation, which supported this research via Grants Nos. AST82-13292 and AST82-16717 to Princeton University.

APPENDIX A: DESCRIPTION OF THE DATA

a) The Data Base

The H I data used in this paper were taken from the literature published since 1975. In many cases, the authors do not list the quantities which we use in our analysis (integrated H I line flux, rms noise of the observations), but these can usually be found by reversing the calculations in each paper. We are reasonably confident that we can do this correctly, with the exception of a survey of southern radio ellipticals made at Parkes by Jenkins (1983), and this sample is therefore not included in the present analysis. However, Jenkins' observations seem to cover the same sensitivity range as the observations in our sample, so their inclusion would not be likely to change our conclusions substantially. The data are presented in Table II. We list first the data for the detections, followed by those for the upper limits. The quantities given in Table II are:

Column (1). The object's catalogue name, from the NGC, the IC, or the UGC (Nilson 1973).

Column (2). The galaxy's revised Hubble type, from the RC2.

Column (3). The galaxy's heliocentric velocity. This is taken from the Revised Shapley-Ames catalogue (Sandage 1981; hereafter referred to as RSA) or from the Harvard redshift survey (Huchra 1984). These redshifts are used to calculate the distance to the galaxy. For some of the detected galaxies, we quote not the galaxy's own redshift but that of the group to which it belongs, as follows:

(i) NGC 1052: The mean group velocity of 1449 km/s is taken from Knapp, Gallagher, and Faber (1978).

(ii) NGC 3265: The mean velocity for the group members (NGC 3265, 3245, 3254, and 3277), listed by Lake and Schommer (1984) is 1394 km/s.

(iii) NGC 3522: The mean velocity of 1124 km/s is for the group members NGC 3522, 3501, and 3507 as listed by Lake and Schommer (1984).

(iv) NGC 3608: The mean velocity of Lake and Schommer's (1984) group members (NGC 3608, NGC 3599, NGC 3605, and NGC 3607) is 911 km/s.

(v) NGC 3998: The members of this group which have measured redshifts are NGC 3998, 3990, 3972, 3982, 3992, and 3953, giving a mean redshift of 960 km/s.

(vi) NGC 4278: The group redshift of 800 km/s is taken from Gallagher *et al.* (1977).

(vii) NGC 5173: The mean redshift for the three members of this group with measured redshifts (see Knapp and Raimond 1984) is 2439 km/s.

(viii) NGC 5576: The group members listed by Lake and Schommer (1984) (NGC 5576, 5636, 5566, 5574, and 5577) have a mean velocity of 1570 km/s.

Column (4). The galaxy's distance. This is usually calculated from the galaxy's redshift. Most of the galaxies in the sample are fairly nearby and their observed redshifts are strongly affected by the local distortion in the Hubble flow caused by the Local Supercluster. Thus, a fairly lengthy series of corrections must be applied to the observed velocities before they can be related to distance. The recipes which we used are described in Appendix B. We took the distances to NGC 205 and NGC 185 to be 0.7 Mpc, the distance to M31. For NGC 5128, we used the recent distance estimate of 2 Mpc by Davies *et al.* (1984). Galaxies within 7° of M87 were assumed to lie at the distance of the Virgo cluster, taken as 13.5 Mpc (see Appendix B).

Column (5). The galaxy's blue magnitude B_T^0, corrected for redshift and extinction by Galactic dust according to the prescriptions in the RC2. Where available, these values are taken directly from the RC2. Otherwise, magnitudes m_z were taken from the Zwicky catalogue [Zwicky *et al.* (1961–1968)]. These were converted to B_T via two empirical relationships. If $m_z > 13^{\rm m}.5$, Bothun and Schommer's (1982) relationship between B_T and m_z was used. If $m_z < 13^{\rm m}.5$, the correction $\Delta m = -0^{\rm m}.29$ recommended by Tonry and Davis (1981a) was used. This intermediate magnitude was then corrected to B_T^0. These estimates of B_T^0 are also listed in column 5, and are indicated by a "z". The magnitude for NGC 5128 is taken from Davies *et al.* (1984), while that for NGC 4105/NGC 4106 is the combined magnitude of the two galaxies.

Column (6). The absolute blue magnitude M_B, found from the distance and the apparent magnitude in columns 4 and 5.

Column (7). The blue luminosity of the galaxy in $L_\odot$ calculated from M_B and a solar blue absolute magnitude of $+5^{\rm m}.48$ (Allen 1973).

Column (8). The listing of the H I data begins here. This column contains the rms noise of the H I observation in mJy.

Column (9). Contains for the detected galaxies the integrated H I line flux $\Sigma S\Delta V$ in Jy × km/s. For the undetected galaxies, we list the 3σ upper limit to this quantity, and this requires an assumed linewidth. This linewidth was scaled to the galaxy's luminosity as described in Appendix C [using equation (C1)]. It was assumed in calculating the upper limit given in column 9 that the gas structure is edge-on, giving the maximum linewidth.

Column (10). Here we list the linewidth observed for the detected galaxies and assumed for the upper limits. The

TABLE II. Observations of H I in elliptical galaxies.

(1) Galaxy	(2) Type	(3) $V_\odot$ (km/sec)	(4) D (Mpc)	(5) m_B	(6) M_B	(7) $L_B(L_\odot)$	(8) HI(rms) (mJy)	(9) HI flux (Jy.km/s)	(10) ΔV km/sec	(11) M_{HI} ($M_\odot$)	(12) M_{HI}/L_B ($M_\odot/L_\odot$)	(13) Ref
N0185	E3p	-245	0.7	9.51	-14.72	1.20(8)	2.2	1.51	25	1.75(5)	0.0015	4
								0.17		1.91(4)	0.0002	
N0205	E5p	-239	0.7	8.44	-15.79	3.21(8)	4.0	3.29	36	3.80(5)	0.0012	4
								0.43		5.00(4)	0.0002	
N1052	E4	1449	13.3	11.21	-19.41	9.03(9)	2.0	8.00	500	3.34(8)	0.0370	17
								3.00		1.25(8)	0.0139	
N1349	E/S0	6593	64.4	14.13z	-19.91	1.44(10)	1.0	2.46	404	2.41(9)	0.1674	12
								1.21		1.19(9)	0.0825	
N3265	E4	1396	19.3	12.97z	-18.46	3.76(9)	0.6	1.79	188	1.57(8)	0.0419	3
								0.36		3.12(7)	0.0083	
N3522	E	1124	10.4	13.14z	-16.95	9.33(8)	0.5	1.08	245	2.76(7)	0.0295	3
								0.35		8.82(6)	0.0094	
N3608	E2	911	8.2	11.70	-17.87	2.19(9)	0.3	0.21	141	3.33(6)	0.0015	3
								0.13		2.01(6)	0.0009	
N3998	S0/E2p	960	15.0	11.27	-19.61	1.09(10)	2.0	6.40	580	3.40(8)	0.0313	1
								3.48		1.85(8)	0.0170	
N4105/6	E3-S0	2044	22.8	11.22	-20.57	2.63(10)	5.0	11.70	760	1.44(9)	0.0546	7
								11.40		1.40(9)	0.0532	
N4278	E1	800	7.9	10.95	-18.54	4.05(9)	2.0	10.96	415	1.61(8)	0.0399	11
								2.49		3.67(7)	0.0091	
N4594	Sa	1128	9.6	8.74	-21.17	4.58(10)	1.2	16.00	754	3.48(8)	0.0076	22
								2.71		5.90(7)	0.0013	
N5128	S0p/I0	541	2.0	6.70	-19.81	1.30(10)	30.0	86.50	536	8.17(7)	0.0063	14
								48.24		4.55(7)	0.0035	
N5173	E0:	2439	30.1	12.96	-19.43	9.23(9)	1.4	4.74	150	1.01(9)	0.1098	2
								0.63		1.35(8)	0.0146	
N5363	I0/Ep	1125	10.8	10.82	-19.35	8.53(9)	0.6	1.89	600	5.20(7)	0.0061	8
								1.08		2.97(7)	0.0035	
N5506	Sap	1753	22.7	12.10z	-19.68	1.16(10)	5.1	9.10	300	1.11(9)	0.0955	8
								4.59		5.58(8)	0.0482	
N5576	E3	1570	21.5	11.47	-20.19	1.86(10)	0.4	0.27	228	2.95(7)	0.0016	3
								0.30		3.28(7)	0.0018	
N5666	comp	2223	27.6	12.90z	-19.30	8.20(9)	0.8	3.68	184	6.62(8)	0.0807	3
								0.41		7.44(7)	0.0091	
A1230+09	E1	1317	13.5	15.01z	-15.64	2.81(8)	0.9	1.49	54	6.41(7)	0.2281	3
								0.15		6.27(6)	0.0223	
I0989	E	7570	79.0	13.28z	-21.21	4.73(10)	0.3	0.54	278	7.95(8)	0.0168	6
								0.29		4.30(8)	0.0091	
I5315	Ecomp	4437	45.2	13.59z	-19.69	1.16e(10)	0.8	0.99	195	4.77(8)	0.0410	12
								0.47		2.26(8)	0.0194	
U01503	E	5087	51.3	13.24z	-20.31	2.07(10)	1.4	1.71	298	1.06(9)	0.0513	12
								1.25		7.77(8)	0.0375	
U06777	E	6999	73.7	15.10z	-19.24	7.71(9)	1.5	2.07	285	2.65(9)	0.3443	12
								1.28		1.64(9)	0.2133	

TABLE II. (continued)

(1) Galaxy	(2) Type	(3) $V_\odot$ (km/sec)	(4) D (Mpc)	(5) m_B	(6) M_B	(7) $L_B(L_\odot)$	(8) HI(rms) (mJy)	(9) HI flux (Jy.km/s)	(10) ΔV km/sec	(11) M_{HI} ($M_\odot$)	(12) M_{HI}/L_B ($M_\odot/L_\odot$)	(13) Ref
U07354	E3?	1582	14.6	13.58z	-17.24	1.23(9)	1.3	2.01	46	1.01(8)	0.0824	3
								0.17		8.68(6)	0.0071	
N0227	E3	5315	51.8	12.26z	-21.31	5.21(10)	9.0	<18.57	(687)	<1.18(10)	<0.2258	23
N0380	E2	4341	44.0	13.12	-20.10	1.70(10)	1.9	< 2.71	(475)	<1.24(9)	<0.0728	16
N0507	S0	4929	49.8	11.76	-21.73	7.63(10)	2.0	< 4.68	(780)	<2.74(9)	<0.0359	16
N0524	S0/E1	2470	24.2	11.24	-20.68	2.91(10)	0.8	< 1.36	(567)	<1.88(8)	<0.0065	16
N0584	E4	1811	17.0	11.06	-20.09	1.69(10)	4.0	< 5.70	(474)	<3.89(8)	<0.0229	21
N0636	E3	1941	18.2	12.05	-19.25	7.80(9)	3.0	< 3,31	(367)	<2.59(8)	<0.0332	23
N0720	E5	1808	16.6	10.89	-20.21	1.89(10)	3.0	< 4.43	(492)	<2.88(8)	<0.0153	21
N0741	E0	5559	54.2	11.98	-21.69	7.38(10)	1.1	< 2.55	(771)	<1.77(9)	<0.0239	16
N0821	E6	1778	17.5	11.51	-19.71	1.19(10)	0.7	< 0.89	(422)	<6.41(7)	<0.0054	16
N0890	S0/E	4043	40.9	11.76z	-21.30	5.15(10)	2.8	< 5.76	(685)	<2.27(9)	<0.0442	16
N1004	E	6480	63.1	13.12z	-20.88	3.50(10)	0.4	< 0.76	(603)	<7.14(8)	<0.0204	6
N1209	E6	2563	23.7	12.03	-19.84	1.35(10)	7.0	< 9.25	(440)	<1.23(9)	<0.0910	23
N1332	S0/E7	1564	13.9	10.84	-19.88	1.39(10)	9.4	<12.54	(444)	<5.72(8)	<0.0412	20
N1407	E0	1811	16.4	10.51	-20.56	2.62(10)	19.0	<31.24	(548)	<1.98(9)	<0.0758	23
N1453	E2	3906	37.4	12.20	-20.66	2.87(10)	10.0	<16.95	(565)	<5.60(9)	<0.1950	23
N1587	E1p	3890	37.6	12.49z	-20.39	2.22(10)	0.2	< 0.31	(519)	<1.04(8)	<0.0047	6
N1600	E3	4830	46.6	11.62	-21.72	7.60(10)	9.0	<21.04	(779)	<1.08(10)	<0.1419	23
N1700	E4	3976	38.3	11.37	-21.55	6.46(10)	4.0	< 8.86	(738)	<3.07(9)	<0.0475	21
N2314	E3	3861	42.2	12.39	-20.74	3.07(10)	4.0	< 6.93	(577)	<2.91(9)	<0.0950	21
N2534	E1p	3549	38.8	12.34z	-20.60	2.71(10)	10.0	<16.64	(554)	<5.91(9)	<0.2179	23
N2672	E1	4223	44.2	12.28	-20.95	3.72(10)	1.3	< 2.40	(615)	<1.11(9)	<0.0297	16
N2693	E3	4956	52.8	12.37	-21.24	4.89(10)	8.0	<16.17	(673)	<1.06(10)	<0.2176	23
N2749	E3	4000	44.5	12.70	-20.54	2.56(10)	0.9	< 1.47	(544)	<6.87(8)	<0.0268	15
N2768	E6	1408	18.6	10.60	-20.75	3.10910)	4.0	< 6.95	(579)	<5.68(8)	<0.0183	21
N2783	E	6713	69.5	12.53z	-21.68	7.31(10)	0.2	< 0.55	(769)	<6.31(8)	<0.0086	6
N2784	S0/E8	708	5.7	10.58	-18.20	2.96(9)	9.9	< 7.93	(267)	<6.08(7)	<0.0205	20
N2855	S0/E1	1901	20.7	12.06	-19.52	1.00(10)	9.9	<11.85	(399)	<1.20(9)	<0.1199	20
N2880	S0/E3	1514	19.8	12.16	-19.32	8.34(9)	2.7	< 3.04	(375)	<2.82(8)	<0.0338	18
N2974	E4/S0	1998	22.5	11.46	-20.30	2.05(10)	3.0	< 4.55	(505)	<5.44(8)	<0.0265	7
N3115	S0/E6	698	5.1	9.70	-18.84	5.34(9)	7.5	< 7.30	(324)	<4.48(7)	<0.0084	20
N3156	S0/E5p	1174	14.9	12.27z	-18.60	4.27(9)	0.9	< 0.81	(301)	<4.26(7)	<0.0100	16
N3193	E2	1371	18.6	11.63	-19.72	1.20(10)	0.7	< 0.89	(423)	<7.27(7)	<0.0061	16
N3377	E5	718	6.0	10.85	-18.04	2.56(9)	0.3	< 0.23	(254)	<1.95(6)	<0.0008	15
N3379	E1	885	7.6	10.00	-19.40	8.99(9)	0.8	< 0.92	(385)	<1.26(7)	<0.0014	16
N3412	S0/E	861	7.4	11.15	-18.20	2.95(9)	0.8	< 0.64	(266)	<8.28(6)	<0.0028	16
N3489	S0/E6	695	5.8	10.81	-18.01	2.48(9)	1.4	< 1.06	(251)	<8.40(6)	<0.0034	16
N3585	E7	1491	17.1	10.64	-20.52	2.52(10	13.0	<21.12	(541)	<1.46(9)	<0.0578	20
N3599	S0	850	7.6	12.52z	-16.88	8.82(8)	0.5	< 0.28	(179)	<3.88(6)	<0.0044	3
N3605	E4	693	6.0	12.22z	-16.67	7.25(8)	0.4	< 0.20	(167)	<1.71(6)	<0.0024	15
N3607	S0/E1	933	8.4	10.73	-18.89	5.60(9)	3.3	< 3.26	(329)	<5.43(7)	<0.0097	13
N3610	E5	1765	23.0	11.33	-20.48	2.42(10	2.7	< 4.33	(534)	<5.40(8)	<0.0223	18
N3640	E3	1354	12.0	11.03	-19.37	8.68(9)	0.6	< 0.74	(380)	<2.52(7)	<0.0029	3
N3641	dE1	1331	11.8	13.78	-16.58	6.66(8)	0.6	< 0.29	(163)	<9.50(6)	<0.0142	3
N3818	E5	1498	13.2	12.45	-18.15	2.84(9)	10.0	< 7.90	(263)	<3.25(8)	<0.1144	23

TABLE II. (continued)

(1) Galaxy	(2) Type	(3) V_0 (km/sec)	(4) D (Mpc)	(5) m_B	(6) M_B	(7) $L_B(L_\odot)$	(8) HI(rms) (mJy)	(9) HI flux (Jy.km/s)	(10) ΔV km/sec	(11) M_{HI} ($M_\odot$)	(12) M_{HI}/L_B ($M_\odot/L_\odot$)	(13) Ref
N3872	E5	3109	35.4	12.41	-20.34	2.12(10)	1.9	< 2.91	(511)	<8.62(8)	<0.0407	10
N3904	E2	1613	18.5	11.59	-19.75	1.23(10)	3.0	< 3.85	(427)	<3.11(8)	<0.0252	7
N3962	E1	1822	22.3	11.27	-20.47	2.40(10)	5.0	< 7.99	(532)	<9.38(8)	<0.0391	7
N4125	E6p	1339	18.9	10.42	-20.96	3.78(10)	8.0	<14.85	(618)	<1.25(9)	<0.0332	23
N4150	S0/E2	244	4.8	12.20	-16.21	4.73(8)	0.5	< 0.22	(145)	<1.19(6)	<0.0025	15
N4179	S0/E8	1279	11.4	11.35	-18.93	5.83(9)	1.9	< 1.90	(334)	<5.84(7)	<0.0100	16
N4239	E	955	13.5	13.01z	-17.64	1.77(9)	0.5	< 0.32	(225)	<1.37(7)	<0.0077	3
N4272	E1	8462	88.4	13.02z	-21.71	7.53(10)	0.2	< 0.56	(776)	<1.03(9)	<0.0137	6
N4274	Sab	722	7.2	10.69	-18.60	4.27(9)	15.0	<13.56	(301)	<1.66(8)	<0.0388	20
N4281	S0/E5	2602	30.7	11.78	-20.66	2.85(10)	3.3	< 5.58	(563)	<1.24(9)	<0.0436	13
N4308	E1	606	13.5	13.29z	-17.36	1.37(9)	0.5	< 0.34	(207)	<1.44(7)	<0.0105	3
N4339	E0	1278	13.5	12.13	-18.52	3.99(9)	3.1	< 2.74	(294)	<1.18(8)	<0.0296	13
N4340	S0	893	13.5	11.91z	-18.74	4.88(9)	13.0	<12.28	(314)	<5.28(8)	<0.1082	19
N4365	E3	1177	13.5	10.39	-20.26	1.98(10)	0.6	< 0.85	(499)	<3.68(7)	<0.0019	5
N4374	E1	933	13.5	10.11	-20.54	2.56(10)	1.8	< 2.94	(544)	<1.26(8)	<0.0049	16
N4382	S0	773	13.5	9.82	-20.83	3.35(10)	0.6	< 1.02	(594)	<4.37(7)	<0.0013	5
N4387	E5	511	13.5	12.75	-17.90	2.25(9)	0.5	< 0.37	(244)	<1.57(7)	<0.0070	15
N4406	E3	-341	13.5	9.93	-20.72	3.02(10)	2.8	< 4.83	(574)	<2.08(8)	<0.0069	13
N4434	E0	1067	13.5	12.69z	-17.96	2.38(9)	0.9	< 0.66	(248)	<2.82(7)	<0.0119	3
N4435	S0/E4	869	13.5	11.42	-19.23	7.67(9)	3.2	< 3.51	(365)	<1.51(8)	<0.0197	13
N4458	E0	383	13.5	12.70	-17.95	2.36(9)	0.6	< 0.45	(247)	<1.92(7)	<0.0081	15
N4459	S0/E2	1111	13.5	11.07	-19.58	1.06(10)	3.7	< 4.51	(406)	<1.94(8)	<0.0183	18
N4468	S0:	895	13.5	13.13z	-17.52	1.59(9)	0.4	< 0.29	(217)	<1.23(7	<0.0078	3
N4472	E2	914	13.5	9.10	-21.55	6.50(10)	0.6	< 1.33	(739)	<5.73(7)	<0.0009	5
N4473	E5	2279	13.5	10.81	-19.84	1.34(10)	3.8	< 5.02	(440)	<2.16(8)	<0.0160	13
N4474	S0p/E6	1526	13.5	12.28	-18.37	3.47(9)	1.9	< 1.60	(281)	<6.90(7)	<0.0199	16
N4477	S0	1263	13.5	11.12	-19.53	1.01(10)	2.5	< 2.98	(400)	<1.28(8)	<0.0127	10
N4478	E2	1482	13.5	11.92	-18.73	4.84(9)	2.1	< 1.98	(314)	<8.51(7)	<0.0176	16
N4489	E1	1019	13.5	12.70z	-17.95	2.36(9)	0.4	< 0.33	(247)	<1.41(7)	<0.0060	3
N4494	E1	1307	12.9	10.54	-20.01	1.57(10)	8.0	<11.13	(463)	<4.37(8)	<0.0277	20
N4526	S0/E7	450	13.5	10.18	-20.47	2.40(10)	0.6	< 0.91	(532)	<3.92(7)	<0.0016	5
N4546	S0/E6	1014	8.7	11.00	-18.70	4.69(9)	2.4	< 2.24	(310)	<4.00(7)	<0.0085	18
N4550	S0/E7	350	13.5	11.90	-18.75	4.93(9)	1.5	< 1.42	(315)	<6.12(7)	<0.0124	16
N4551	E3	978	13.5	12.65	-18.00	2.47(9)	2.4	< 1.81	(251)	<7.79(7)	<0.0315	13
N4552	E0	239	13.5	10.62	-20.03	1.60(10)	0.5	< 0.70	(466)	<3.01(7)	<0.0019	15
N4564	E6/S0	1020	13.5	11.68	-18.97	6.03(9)	0.6	< 0.58	(337)	<2.48(7)	<0.0041	5
N4612	S0/Ep	1832	13.5	12.38z	-18.27	3.17(9)	3.9	< 3.19	(273)	<1.37(8)	<0.0434	13
N4621	E5	414	13.5	10.55	-20.10	1.71(10)	0.6	< 0.81	(476)	<3.50(7)	<0.0020	5
N4623	S0/E5	1788	13.5	12.16z	-18.49	3.88(9)	1.5	< 1.31	(291)	<5.65(7)	<0.0146	3
N4636	E0	939	8.3	10.29	-19.31	8.21(9)	0.6	< 0.64	(373)	<1.04(7)	<0.0013	5
N4649	E2	1200	13.5	9.62	-21.03	4.02(10)	1.6	< 3.03	(631)	<1.30(8)	<0.0032	16
N4660	E5	1017	13.5	11.63	-19.02	6.32(9)	3.4	< 3.50	(342)	<1.50(8)	<0.0238	13
N4697	E6	1308	11.7	9.96	-20.38	2.21(10)	3.0	<20.22	(518)	<6.53(8)	<0.0296	20
N4753	I0	1255	11.4	10.43	-19.85	1.36(10)	3.0	<17.23	(441)	<5.28(8)	<0.0388	20
N4754	S0/E	1461	13.5	11.17	-19.48	9.65(9)	8.9	<10.53	(394)	<4.53(8)	<0.0469	20
N4839	S0	7446	78.4	12.09z	-22.38	1.40(11)	0.6	< 1.71	(952)	<2.49(9)	<0.0178	15

TABLE II. (continued)

(1) Galaxy	(2) Type	(3) $V_\odot$ (km/sec)	(4) D (Mpc)	(5) m_B	(6) M_B	(7) $L_B(L_\odot)$	(8) HI(rms) (mJy)	(9) HI flux (Jy.km/s)	(10) ΔV km/sec	(11) M_{HI} ($M_\odot$)	(12) M_{HI}/L_B ($M_\odot/L_\odot$)	(13) Ref
N4853	S0	7550	79.5	13.69	-20.81	3.29(10)	0.9	< 1.60	(590)	<2.38(9)	<0.0724	15
N4874	E0	7176	75.8	12.60	-21.80	8.15(10)	1.0	< 2.39	(797)	<3.24(9)	<0.0398	15
N4880	E4/S0	1557	13.5	12.80z	-17.85	2.15(9)	2.1	< 1.51	(240)	<6.51(7)	<0.0303	15
N4889	E4	6467	68.8	12.16	-22.03	1.01(11)	0.6	< 1.54	(855)	<1.72(9)	<0.0171	15
N5077	E3	2823	31.8	12.32	-20.19	1.86(10)	3.0	< 4.41	(489)	<1.05(9)	<0.0566	23
N5273	S0/E1p	1022	10.9	12.20	-17.99	2.44(9)	2.2	< 1.65	(250)	<4.63(7)	<0.0190	16
N5322	E3	1902	24.7	10.57	-21.39	5.62(10)	4.0	< 8.46	(705)	<1.22(9)	<0.0217	7
N5576	E3	1528	15.0	11.47	-19.41	9.04(9)	0.9	< 1.04	(385)	<5.53(7)	<0.0061	16
N5638	E1	1677	22.3	11.90	-19.84	1.34(10)	1.5	< 1.98	(440)	<2.32(8)	<0.0173	16
N5812	E0	2066	24.9	11.83	-20.15	1.79(10)	4.0	< 5.80	(483)	<8.49(8)	<0.0475	21
N5813	E	1882	23.8	11.30	-20.58	2.66(10)	0.7	< 1.22	(551)	<1.64(8)	<0.0061	3
N5831	E3	1684	21.9	12.10	-19.60	1.08(10)	0.6	< 0.70	(409)	<7.92(7)	<0.0073	3
N5838	S0	1427	19.4	11.37	-20.07	1.66(10)	9.9	<14.00	(471)	<1.24(9)	<0.0750	20
N5845	E3	1557	20.7	12.35z	-19.23	7.65(9)	0.6	< 0.62	(365)	<6.32(7)	<0.0083	3
N5846	E0	1713	22.1	10.89	-20.83	3.35(10)	0.8	< 1.50	(594)	<1.73(8)	<0.0052	3
N5846A	dE2	1713	22.1	13.84	-17.88	2.21(9)	3.0	< 2.18	(242)	<2.52(8)	<0.1138	3
N5982	E3	2879	34.0	11.75	-20.91	3.59(10)	8.0	<14.60	(608)	<3.98(9)	<0.1110	3
N6482	E3	3922	43.1	11.59	-21.58	6.68(10)	3.0	< 6.72	(746)	<2.95(9)	<0.0441	3
N6702	E3	4725	51.2	12.68	-20.87	3.46(10)	10.0	<18.02	(600)	<1.12(10	<0.3227	3
N6946	E4p	3832	39.4	13.12	-19.86	1.36(10)	5.0	< 6.63	(442)	<2.43(9)	<0.1781	3
N7052	E4	4920	51.1	12.24z	-21.30	5.16(10)	0.2	< 0.33	(685)	<2.03(8)	<0.0039	6
N7274	E0	5826	60.0	12.68z	-21.21	4.75(10)	9.0	<18.01	(667)	<1.53(10	<0.3225	23
N7317	E2	6736	68.8	14.01	-20.18	1.83(10)	0.7	< 1.02	(487)	<1.14(9)	<0.0624	16
N7436	E	7409	74.9	12.56z	-21.81	8.26(10)	0.2	< 0.38	(800)	<5.09(8)	<0.0062	6
N7457	S0/Ep	525	7.6	11.20	-18.20	2.98(9)	0.6	< 0.48	(267)	<6.56(6)	<0.0022	15
N7557	E2/S0	3612	36.1	14.29z	-18.50	3.90(9)	3.5	< 3.07	(292)	<9.44(8)	<0.2422	9
N7562	E2	3806	38.0	12.28	-20.62	2.75(9)	7.0	<11.70	(557)	<3.99(9)	<0.1450	23
N7617	S0	4072	40.6	14.38	-18.66	4.54(9)	3.3	< 3.04	(307)	<1.18(9)	<0.2609	9
N7619	E2	3757	37.5	11.78	-21.09	4.25(10)	0.7	< 1.27	(643)	<4.23(8)	<0.0100	5
N7626	E1p	3439	34.4	11.94	-20.74	3.08(10)	0.7	< 1.15	(578)	<3.20(8)	<0.0104	5
N7728	E	9498	95.4	13.05z	-21.85	8.53(10)	0.2	< 0.58	(809)	<1.25(9)	<0.0147	6
N7785	E5	3846	38.0	12.31	-20.59	2.68(10)	0.7	< 1.09	(552)	<3.73(8)	<0.0139	5
I0948	E	6912	72.9	13.32z	-20.99	3.89(10)	0.2	< 0.30	(624)	<3.76(8)	<0.0097	6
I3413	E4?	1019	13.5	14.70z	-15.95	3.74(8)	0.5	< 0.22	(134)	<9.40(6)	<0.0251	3
I3442	E0:	1019	13.5	15.03z	-15.62	2.76(8)	0.9	< 0.32	(122)	<1.39(7)	<0.0502	3
I3475	E3:	1029	13.5	15.03z	-15.62	2.76(8)	0.7	< 0.27	(122)	<1.17(7)	<0.0422	3
I3773	dE	1095	13.5	13.28z	-17.37	1.38(9)	0.5	< 0.29	(207)	<1.26(7)	<0.0091	3
U01308	E	5173	52.3	13.38z	-20.21	1.89(10)	0.7	< 0.99	(492)	<6.39(8)	<0.0338	6

References to TABLE II.

[1]Knapp, van Driel, and van Woerden 1984.
[2]Knapp and Raimond 1984.
[3]Lake and Schommer 1984.
[4]Johnson and Gottesmann 1983.
[5]Thonnard 1983.
[6]Dressel, Bania, and O'Connell 1982.
[7]Knapp and Gunn 1982.
[8]Thuan and Wadiak 1982.
[9]Richter and Huchtmeier 1982.
[10]Helou *et al.* 1981.
[11]Raimond *et al.* 1981.
[12]Haynes and Giovanelli 1980.
[13]Krumm and Salpeter 1979.
[14]Gardner and Whiteoak 1976.
[15]Knapp, Kerr, and Henderson 1979.
[16]Knapp, Kerr, and Williams 1978.
[17]Reif *et al.* 1978.
[18]Bieging 1978.
[19]Huchtmeier *et al.* 1976.
[20]Gallagher, Faber, and Balick 1975.
[21]Shostak, Roberts, and Peterson 1975.
[22]Bajaja *et al.* 1984.
[23]Gallagher *et al.* 1984.

width for the observed H I lines is the velocity difference between the 50% power points.

Column (11). Gives the H I mass or its upper limit in $M_\odot$, calculated from equation (1). The upper limits for the nondetections are 3σ values. For the detections, we list below each value of M(H I) the amount of H I which could have been detected by the observations, again at the 3σ level, to be directly comparable with the upper limits for the nondetected galaxies. Indeed, a couple of the detections in Table II are near the 3σ level. The linewidth assumed in calculating these minimum H I masses is the observed value.

Column (12). Lists the value of M(H I)/L_B or its upper limit.

Column (13). Lists the reference from which the H I data were taken. The references are given in the notes to Table I.

Since the amounts of H I in ellipticals are small, there is often doubt about the reality of a detection. The observations for some of the individual galaxies are now discussed briefly.

b) Elliptical Galaxies Containing H I

(1). NGC 185. H I emission from this Local Group dwarf elliptical galaxy has been detected with the VLA by Johnson and Gottesman (1983) at a level of 1.5 Jy km/s. This is not in conflict with Thuan and Seitzer's (1979) upper limit with the NRAO 91-m telescope of $\sim$4 Jy km/s, but is marginally inconsistent with the upper limit of 0.6 Jy km/s, also set by the 91 m, of Gallagher *et al.* (1984). The single-dish observations, however, may be affected by strong emission from M31. The H I in NGC 185 seems to be in a single small cloud, coincident neither with the center of NGC 185 nor with the dust patches seen in the galaxy.

(2). NGC 205. The detection of H I in this second Local Group dwarf has been made by Warner and Baldwin (reported by Unwin 1980) and by Johnson and Gottesman (1983), again with the VLA. This galaxy contains dust and young stars, but the H I emission is not coincident with the dust. The H I emission strength found by both groups is similar.

(3). NGC 1052. H I emission from this active galaxy was first detected at Parkes by Whiteoak and Gardner (1977). Their observation was probably somewhat confused by emission from the nearby spiral NGC 1042, and was in conflict with the upper limit set at the NRAO 91 m by Shostak, Roberts, and Peterson (1975). However, subsequent observations with several telescopes (Knapp, Gallagher, and Faber 1978; Fosbury *et al.* 1978; Reif *et al.* 1978; Bottinelli and Gouguenheim 1980) have confirmed the presence of H I in this elliptical. The integrated fluxes reported by these authors do no agree very well, for at least two reasons. The first is varying degrees of contamination by the strong emission from NGC 1042, and the second the increasing strength of the absorption caused by the increasing strength of the compact nuclear continuum source (van Gorkom *et al.* 1984). The value of the integrated H I flux given in Table II represents a compromise among values in the literature.

(4). NGC 1349, UGC 1503, UGC 6777 and IC 5315. These four isolated early-type galaxies were strongly detected in the H I line by Haynes and Giovanelli (1980) and the parameters listed in Table II are from this reference. Of these galaxies, three are classified as ellipticals and the fourth, NGC 1349, as an E/SO. The fifth isolated early-type galaxy detected by Haynes and Giovanelli, IC 1861, is classified as SO and is not included in the present study. These galaxies are all fairly distant, and their classification is therefore uncertain.

(5). NGC 3265, NGC 3522, NGC 3608, NGC 5576, and UGC 07354. These galaxies are all dwarf ellipticals detected at Arecibo by Lake and Schommer (1984). Two other possible detections in this work (NGC 4318, NGC 4551) are not included here because the possible H I emission features are at velocities different from the optically measured velocities of the galaxies. These galaxies, having faint apparent magnitudes, have uncertain classifications, and one or two of them may be blue compact galaxies. For NGC 3265, NGC 3522, and A1230 + 09, only the Lake and Schommer H I observations exist. The marginal detection of NGC 3608 at a level of 0.21 Jy km/s is not in disagreement with the Arecibo upper limit of 4 Jy km/s of Krumm and Salpeter (1979). NGC 5576 is also a marginal detection at 0.27 Jy km/s, which does not conflict with the upper limit of 0.6 Jy km/s found by Knapp, Kerr, and Williams (1978). The H I observation of NGC 5666 is in good agreement with the 91-m detection of this galaxy by Peterson (1979). This galaxy's type is "compact", however, and it may not be a true elliptical. A1230 + 09 is strongly detected. UGC 07354 is likewise strongly detected, and the H I observation is in good agreement with those of Gordon and Gottesman (1981) and Thuan and Martin (1981), though, again, the galaxy's "blue compact" morphology renders its type uncertain.

(6). NGC 3998. After several failures to detect H I in this active galaxy (Gallagher, Faber, and Balick 1975; Knapp *et al.* 1977; Appleton and Davies 1982), Gallagher *et al.* (1984) reported a possible weak detection which was confirmed by synthesis observations at Westerbork (Knapp, van Driel, and van Woerden 1984). Although the galaxy is often classified as SO, it has enough features in common with active ellipticals (see Knapp, van Driel, and van Woerden 1984) to justify including it in the present data set.

(7). NGC 4105/NGC 4106. Tentative detections of H I in this E/SO pair (Huchtmeier, Tammann, and Wendker 1977; Bottinelli and Gouguenheim 1971a; Balkowski 1979) were confirmed by observations made with a large bandwidth by Knapp and Gunn (1982), who showed that the velocity dispersion of the H I emission is large. There is as yet no information on how the gas is distributed with respect to the two galaxies, both of which are early type and show no signs of dust (Sandage 1981). Here, we calculate M(H I)/L_B by taking the combined luminosity of the two galaxies.

(8). NGC 4278. This galaxy was the first normal elliptical with a well-confirmed H I detection (Bottinelli and Gouguenheim 1977a; Gallagher *et al.* 1977; Bieging 1978; Knapp, Kerr, and Williams 1978; Krumm and Salpeter 1979) and the H I distribution has been mapped at Westerbork (Raimond *et al.* 1981). The galaxy is, with NGC 1052, the prototype of the active, H I-rich elliptical (its properties are discussed more fully in the above references). The parameters used in Table II are those given by Raimond *et al.* (1981).

(9). NGC 4594. This galaxy is, of course, not an elliptical but has many of the features of the class, especially a very large, de Vaucouleurs-law bulge (e.g., Faber *et al.* 1977). As pointed out by Faber *et al.* (1977), its relative H I content is lower than many of the upper limits for ellipticals. Bajaja *et al.* (1984) have shown that the H I ring avoids the bulge, as is the case for ellipticals, e.g., NGC 4278, in which H I has been mapped. We include it here because it is among the most luminous bulge systems in our sample; the H I parameters are taken from Bajaja *et al.* (1984).

(10). NGC 5128. This peculiar galaxy is now reasonably

generally accepted as the product of a merger between an elliptical and a gas-rich system, and as such fits naturally into the present data set. The H I parameters used here are taken from Gardner and Whiteoak (1976) [those of Gosachinskii *et al.* (1980) are in reasonable agreement], but the H I flux is probably underestimated because of strong absorption against the continuum source.

(*11*). *NGC 5173.* This galaxy was tentatively detected in the H I line by Gallagher *et al.* (1984), but the observations were confused by H I emission from the nearby spiral NGC 5169. Synthesis observations (Knapp and Raimond 1984) clearly show H I associated with NGC 5173, and the parameters used in Table II are taken from that paper.

(*12*). *NGC 5363 and NGC 5506.* These are also IO galaxies, with underlying elliptical morphology and almost polar dust lanes. H I emission has been detected in both galaxies by Thuan and Wadiak (1982) and these data are listed in Table II. Both values of the H I flux are probably affected by absorption. NGC 5363 has also been observed by Shostak (1978), Haynes (1981), Haynes and Giovanelli (1981), Bottinelli *et al.* (1982), and Lake and Schommer (1984), and the observations are in reasonable agreement.

(*13*). *IC 989.* A strong detection of H I emission from this distant radio galaxy has been made at Arecibo by Dressell, Bania, and O'Connell (1982).

In addition to the above galaxies, H I emission has been detected in two more systems which may belong to the above class, but are not included in the present sample. These are NGC 520 (Thuan and Wadiak 1982) and NGC 3773 (Knapp, Kerr, and Henderson 1979); both are of very uncertain morphology. H I emission has also been seen at the position of NGC 3226 (Knapp, Kerr, and Williams 1978), but the observation is confused by emission from the neighboring spiral NGC 3227 and this galaxy is therefore not included in the present sample.

c) The Upper Limits

Here, we discuss some of the nondetections in Table II, dealing mostly with galaxies which at one time or another have been suspected of containing H I. Such observational difficulties are inevitable when the amounts of gas are as small as they are in elliptical galaxies.

(*1*). *NGC 4472.* Many searches for H I emission from this galaxy, the most luminous in the Virgo Cluster, have been made, all without success (Huchtmeier, Tammann, and Wendker 1975, 1976; Knapp, Kerr, and Williams 1978; Krumm and Salpeter 1979; Knapp and Gunn 1982; Thonnard 1983). H I emission from a satellite late-type dwarf has been detected by Thonnard (1983). The limit in Table II is taken from Knapp and Gunn (1982). While not the most sensitive observation, this was made with a large enough bandwidth that any emission from the galaxy could be identified.

(*2*). *NGC 4374.* This galaxy, like several of the ellipticals in which H I has been detected, has a dust lane, but sensitive observations made so far have failed to find H I emission (Huchtmeier, Tammann, and Wendker 1977; Roberts and Steigerwald 1977; Knapp, Kerr, and Williams 1978; Krumm and Salpeter 1979).

(*3*). *NGC 1587/1588.* The possible detection by Gallagher, Knapp, and Faber (1981) at the 91-m telescope was not confirmed by more sensitive observations at Arecibo by Dressell, Bania, and O'Connell (1982).

(*4*). *NGC 2974, NGC 3904, NGC 3962.* The H I detections of these galaxies reported by Bottinelli and Gouguenheim (1977b, 1979a,b) and Huchtmeier, Tammann, and Wendker (1975, 1977) were not confirmed in more sensitive observations by Knapp and Gunn (1982).

(*5*). *NGC 4636.* Recent sensitive observations of this galaxy (Thonnard 1983; Gallagher *et al.* 1984) fail to confirm previous H I detections (Huchtmeier, Tammann, and Wendker 1975, 1976; Bottinelli and Gouguenheim 1978; Knapp, Faber, and Gallagher 1978).

(*6*). *NGC 5846.* The detection of H I in this galaxy (Huchtmeier, Tammann, and Wendker 1975, 1977; Bottinelli and Gouguenheim 1979a) is not confirmed by more sensitive observations (Knapp, Kerr, and Williams 1978; Knapp, Kerr, and Henderson 1979; Gallagher *et al.* 1984).

Otherwise, the upper limits in Table II represent the most sensitive observations of a galaxy, where two or more observations exist. Galaxies whose upper limits are larger than the largest observed value of $M_{\rm H\,I}/L_B$ ($0.34\,M_\odot/L_\odot$ for UGC 06777) were removed from the sample.

APPENDIX B: DISTANCES

The distances used in this paper are mostly calculated from the redshifts. Recent studies of the dynamics of the Local Supercluster (Tonry and Davis 1981b; Schechter 1980; Aaronson *et al.* 1982) have shown that the local velocity field is strongly affected by deceleration by the Local Supercluster. The distance of a given galaxy relative to that of the Virgo cluster can be calculated using Schechter's (1980) equation

$$V_0' = V_v' d - w_i(\cos\theta - d)[1 - (d^2 - 2d\cos\theta + 1)^{-\gamma/2}], \quad \text{(B1)}$$

where we take γ, the power law describing the spherically symmetric density distribution in the Local Supercluster, to be 2. In equation (B1), θ is the angle between the direction to the galaxy and that to M87 (taken to be the center of the Local Supercluster), d is the distance to the galaxy in units of the Virgo cluster distance, and w_i is the infall velocity to Virgo at the distance of the Local Group. In addition, a peculiar velocity of the Local Group with respect to this "local standard of rest" may be present. V_v' is the observed velocity of the Virgo cluster corrected for this peculiar motion and for the motion of the Sun and the Galaxy within the Local Group, and V_0' the velocity of the galaxy with the same corrections applied.

Aaronson *et al.* (1982) have provided the most recent and detailed solutions for the Virgocentric flow and for the peculiar velocity of the Local Group with respect to this flow. We have chosen to use a simplified version of their solution, taking only the peculiar velocity component along the direction to M87. Aaronson *et al.*'s solution 3.1 (from their Table I) gives $w_i = 250$ km/s, and the component of the peculiar velocity of the Local Group along this direction, $w_z = 81$ km/s. The prescription for finding distances used in our paper is then: (1). Correct the observed heliocentric velocity $V_\odot$ of the galaxy to the center of mass of the Local Group, after the RC2:

$$V_0 = V_\odot + 300 \sin l \cos b. \quad \text{(B2)}$$

(2). The velocity of the Virgo cluster with respect to the Local Group is given by Mould, Aaronson, and Huchra (1980) as 1019 km/s. This velocity, corrected for an infall velocity of 331 km/s, is then 1350 km/s. Taking $H_0 = 100$ km/s/Mpc

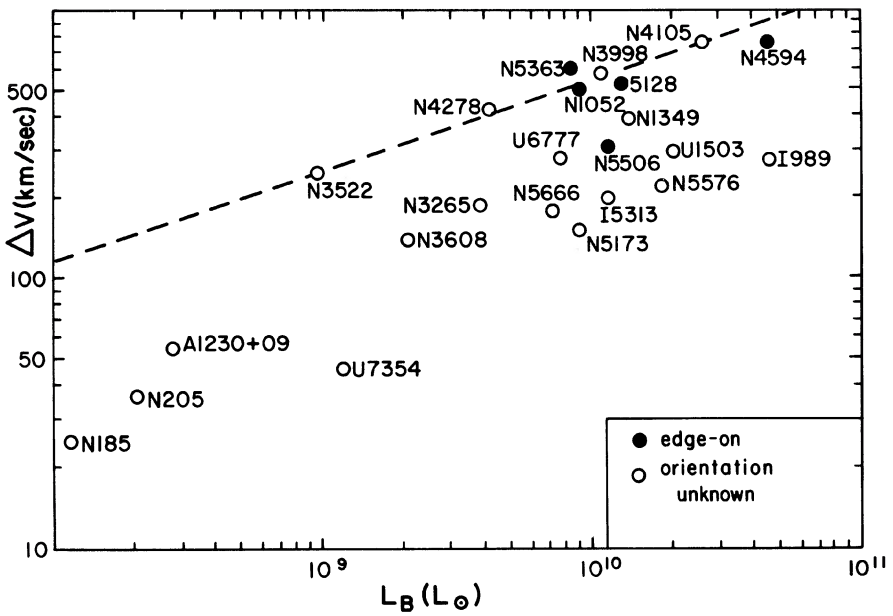

FIG. 10. Plot of ΔV(H I) versus L_B for H I-detected ellipticals. Dark circles correspond to galaxies where the H I disks are likely to be close to edge-on. The dotted line is the assumed $\Delta V - L_B$ relationship (see the text).

gives a distance to the Virgo cluster of 13.5 Mpc. (3). Using the above numbers, equation (B1) now reads

$$V_0 = 1019d - 331\,(\cos\theta - d)[1 - (d^2 - 2d\cos\theta + 1)^{-1}] \quad \text{(B3)}$$

and can be solved for d by iteration. A recipe giving values of d using the full treatment of Aaronson *et al.* (1982) is given by van Driel (1984).

Equation (B3) gives triple-valued distances $0 \lesssim 30°$. We have taken galaxies with $\theta \lesssim 7°$ and $V \leqslant 2500$ km/s to be in the Virgo cluster at 13.5 Mpc distance. For galaxies in our sample with $30° \gtrsim \theta \gtrsim 7°$, we find that the average of the distance values is always near 13.5 Mpc. In any case, Aaronson *et al.* caution against the use of equation (B1) for galaxies between the Local Group and Virgo. Because the projection effects are small with $\theta \lesssim 30°$, we have, for these galaxies, simply divided V_0 by 100 km/s/Mpc if $V_0 < 1000$ km/s. Only six galaxies (UGC 07354, NGC 3607, NGC 4179, NGC 4546, NGC 4636, and NGC 4753) fall into this category, and all except UGC 07354 are undetected in H I. For the remaining galaxies, we find the distance using Equation (B3).

APPENDIX C: LINEWIDTHS

It has been shown observationally (Faber and Jackson 1976; Tully and Fisher 1977) that a proportionality exists between the global velocity dispersion and the luminosity of galaxies. Lake and Schommer (1984) find such a relationship between H I linewidths and luminosities in H I detected galaxies.

In Fig. 10, we show ΔV_{50}, the full velocity width at the 50% power points, versus L_B for the 23 detected galaxies in our sample. Since the inclination of the H I structures is in most cases unknown, we expect any relationship to be revealed by the upper envelope of ΔV_{50}. In Fig. 10, we have indicated those galaxies for which there is evidence that the H I disk is edge-on.

Figure 10 suggests a proportionality between ΔV_{50} and L_B something like

$$\Delta V_{50} \simeq 0.25 \left(\frac{L_B}{L_\odot}\right)^{1/3} \text{km/s} \ , \quad \text{(C1)}$$

which is sketched in Fig. 10. This relationship has been used in estimating the linewidths for the undetected galaxies in Table II.

REFERENCES

Aaronson, M., Huchra, J., Mould, J., Schechter, P. L., and Tully, R. B. (1982). Astrophys. J. **258**, 64.

Allen, C. W. (1973). *Astrophysical Quantities* (Athlone, London).

Appleton, P. N ., and Davies, R. D. (1982). Mon. Not. R. Astron. Soc. **201**, 1073.

Bahcall, J. N. (1980). Astrophys. J. **240**, 377.

Bajaja, E., van der Berg, G., Faber, S. M., Gallagher, J. S., Knapp, G.R., and Shane, W. W. (1984). Astron. Astrophys. (in press).

Balkowski, C. (1979). Astron. Astrophys. **76**, 190.

Bieging, J. (1978). Astron. Astrophys. **64**, 23.

Bothun, G. D., and Schommer, R. A. (1982). Astrophys. J. Lett. **255**, L23.

Bottinelli, L., and Gouguenheim, L. (1977a). Astron. Astrophys. **54**, 641.

Bottinelli, L., and Gouguenheim, L. (1977b). Astron. Astrophys. **60**, L23.

Bottinelli, L., and Gouguenheim, L. (1978). Astron. Astrophys. **64**, L3.

Bottinelli, L., and Gouguenheim, L. (1979a). Astron. Astrophys. **74**, 172.

Bottinelli, L., and Gouguenheim, L. (1979b). Astron. Astrophys. **76**, 176.

Bottinelli, L., and Gouguenheim, L. (1980). Astron. Astrophys. **88**, 108.

Bottinelli, L., Gouguenheim, L., and Paturel, G. (1980). Astron. Astrophys. **88**, 32.

Bottinelli, L., Gouguenheim, L., and Paturel, G. (1982). Astron. Astrophys. Suppl. **50**, 101.

Davies, R.L., Danziger, I. J., Fabian, A., Hanes, R., Jones, B. T. J., Jones, J., Morton, D.C., and Pennington, R. (1984). In preparation.

de Vaucouleurs, G., de Vaucouleurs, A., and Corwin, H. C. (1976). *Second Reference Catalogue of Bright Galaxies* (University of Texas, Austin) (RC2).

Dressell, L. L., Bania, T. M., and O'Connell, R. W. (1982). Astrophys. J. **259**, 55.
Faber, S. M., and Gallagher, J. S. (1976). Astrophys. J. **204**, 365.
Faber, S. M., and Jackson, R. E. (1976). Astrophys. J. **204**, 668.
Faber, S. M. Balick, B., Gallagher, J. S., and Knapp, G. R. (1977). Astrophys. J. **214**, 383.
Felten, J. E. (1976). Astrophys. J. **207**, 700.
Fisher, J. R., and Tully, R. B. (1981). Astrophys. J. Suppl. **47**, 139.
Fosbury, R. A. E., Mebold, U., Goss, W. M., and Dopita, M. A. (1978). Mon. Not. R. Astron. Soc. **183**, 549.
Gallagher, J.S., Faber, S. M., and Balick, B. (1975). Astrophys. J. **202**, 7.
Gallagher, J. S., Knapp, G. R., Faber, S. M., and Balick, B. (1977). Astrophys. J. **215**, 463.
Gallagher, J. S., Knapp, G. R., and Faber, S. M. (1981). Astron. J. **86**, 1781.
Gallagher, J. S., Bushouse, H., Knapp, G. R., and Faber, S. M. (1984). In preparation.
Gardner, F. F., and Whiteoak, J. B. (1976). Proc. Astron. Soc. Aust. **3**, 63.
Gordon, D., and Gottesmann, S. T. (1981). Astron. J. **86**, 161.
Gosachinskii, I. V., Grachev, V. G., and Ryzhkov, N. F. (1981). Sov. Astron.-AJ **24**, 647.
Hawarden, T. G., Elson, R. A. W., Longmore, A. J., Tritton, S. B., and Corwin, H. C. (1981). Mon. Not. R. Astron. Soc. **196**, 747.
Haynes, M. P. (1981). Astron. J. **86**, 1126.
Haynes, M. P., and Giovanelli, R. (1980). Astrophys. J. Lett. **240**, L87.
Haynes, M. P., and Giovanelli, R. (1981). Astrophys. J. Lett. **246**, L105.
Helou, G., Giovanardi, C., Salpeter, E. E., and Krumm, N. (1981). Astrophys. J. Suppl. **46**, 267.
Huchra, J. P. (1984). Private communication.
Huchtmeier, W. K., Tammann, G. A., and Wendker, H. J. (1975). Astron. Astrophys. **42**, 205.
Huchtmeier, W. K., Tammann, G. A., and Wendker, H. J. (1976). Astron. Astrophys. **46**, 381.
Huchtmeier, W. K., Tammann, G. A., and Wendker, H. J. (1977). Astron. Astrophys. **57**, 313.
Huchtmeier, W. K., Richter, O. G., Bohnenstengel, H.-D., and Hauschildt, M. (1983). ESO preprint #250.
Humason, M. L., Mayall, N. U., and Sandage, A. R. (1956). Astron. J. **61**, 97.
Hummel, E. (1980). Ph. D. thesis, University of Groningen.
Hunter, D. A., Gallagher, J. S., and Rautenkranz, D. (1982). Astrophys. J. Suppl. **49**, 53.
Jenkins, C. R. (1983). Mon. Not. R. Astron. Soc. **205**, 1321.
Johnson, D. W., and Gottesmann, S. T. (1983). Astrophys. J. **275**, 549.
Knapp, G. R., van Driel, W., and van Woerden, H. (1984). Astron. Astrophys. (in press).
Knapp, G. R., Faber, S. M., and Gallagher, J. S. (1978). Astron. J. **83**, 11.
Knapp, G. R., Gallagher, J. S., and Faber, S. M. (1978). Astron. J. **83**, 139.
Knapp, G. R., Gallagher, J. S., Faber, S. M., and Balick, B. (1977). Astron. J. **82**, 106.
Knapp, G. R., and Gunn, J. E. (1982). Astron. J. **87**, 1634.
Knapp, G. R., Kerr, F. J., and Henderson, A. P. (1979). Astrophys. J. **234**, 448.
Knapp, G. R., Kerr, F. J., and Williams, B. A. (1978). Astrophys. J. **222**, 800.
Knapp, G. R., and Raimond, E. (1984). Astron. Astrophys. **138**, 77.
Krumm, N., and Salpeter, E. E. (1979). Astrophys. J. **227**, 776.
Lake, G., and Schommer, R. A. (1984). Astrophys. J. **280**, 107.
Lake, G., Schommer, R. A., and van Gorkom, J. (1984). In preparation.
Mould, J., Aaronson, M., and Huchra, J. (1980). Astrophys. J. **238**, 458.
Nilson, P. (1973). *Uppsala General Catalogue of Galaxies*, Acta Uppsaliensis Ser. 5A, Vol. 1(UGC).
Peterson, S. D. (1979). Astrophys. J. Suppl. **40**, 527.
Raimond, E., Faber, S. M., Gallagher, J. S., and Knapp, G. R. (1981). Astrophys. J. **246**, 708.
Reif, K., Mebold, U., and Goss, W. M. (1978). Astron. Astrophys. **67**, L1.
Richter, O.-G., and Huchtmeier, W. K. (1982). Astron. Astrophys. **109**, 155.
Roberts, M. S. (1975). In *Stars and Stellar Systems*, edited by A. R. Sandage, M. Sandage, and J. Kristian (University of Chicago, Chicago), Vol. IX, p. 309.
Roberts, M. S., and Steigerwald, D. C. (1977). Astrophys. J. **217**, 883.
Sandage, A. R. (1981). Private communication.
Sandage, A. R., and Tammann, G. A. (1981). *Revised Shapley-Ames Catalogue of Galaxies* (Carnegie Institution of Washington, Washington, D.C.) (RSA).
Sanders, R. H. (1980). Astrophys. J. **242**, 931.
Schechter, P. L. (1976). Astrophys. J. **203**, 297.
Schechter, P. L. (1980). Astron. J. **85**, 801.
Schmidt, M. (1968). Astrophys. J. **151**, 393.
Shostak, G. S. (1978). Astron. Astrophys. **68**, 321.
Shostak, G. S., Roberts, M. S., and Peterson, S. D. (1975). Astron. J. **80**, 581.
Thonnard, N. (1983). In *Internal Kinematics and Dynamics of Galaxies*, IAU Symposium No. 100, edited by E. Athanassoula (Reidel, Dordrecht), p. 305.
Thuan, T. X., and Martin, G. E. (1981). Astrophys. J. **247**, 823.
Thuan, T. X., and Seitzer, P.O. (1979). Astrophys. J. **231**, 327.
Thuan, T. X., and Wadiak, E. J. (1982). Astrophys. J. **252**, 125.
Tinsley, B. M. (1980). Fundam. Cosmic Phys. **5**, 287.
Tonry, J. L., and Davis, M. (1981a). Astrophys. J. **246**, 666.
Tonry, J. L., and Davis, M. (1981b). Astrophys. J. **246**, 680.
Tully, R. B., and Fisher, J. R. (1977). Astron. Astrophys. **54**, 661.
Turner, E. L. (1985). In preparation.
Unwin, S. C. (1980). Mon. Not. R. Astron. Soc. **190**, 551.
van Driel, W. (1984). In preparation.
van Gorkom, J., van der Hulst, J. M., and Golisch, W. F. (1984). In preparation.
Whiteoak, J. B., and Gardner, F. F. (1977). Aust. J. Phys. **30**, 187.
Zwicky, F., *et al.* (1961–1968). *Catalogue of Galaxies and Clusters of Galaxies* (Carnegie Institute of Washington, Washington, D.C.).